Cellulose (2024) 31:587–605
https://doi.org/10.1007/s10570-023-05612-y

ORIGINAL RESEARCH

Fire performance, toxicity, and thermal diffusivity of wastepaper mixed with magnesium hydroxide, depending on the particle size of expandable graphite

Chansol Ahn · Dongin Park · Yongjoo Kim · Dongho Rie

Received: 27 June 2023 / Accepted: 10 November 2023 / Published online: 9 December 2023

Abstract As the construction of high-rise buildings increases to solve residential spaces caused by high density population concentration, the occurrence of fire accidents in high-rise buildings is also increasing. The primary cause of fire damage in high-rise buildings is the spread of fire caused by exterior wall finishes. Therefore, it is essential to develop semi-non-combustible finishes that can be applied to high-rise buildings to prevent the spread of fire due to exterior wall finishes. To address this issue, numerous studies are being conducted to develop flame retardant finishing materials that reduce heat release rate and total heat release. A double flame retardant mixed waste paper with expandable graphite and magnesium hydroxide was manufactured to improve the fire performance of cellulose building finishing materials. Total heat release (THR), CO, and CO_2 Generation changes were measured using a cone calorimeter, and thermal diffusion rate was measured through the LFA 1000 experiment. The correlation of total heat release, CO generation, CO_2 generation, and mass reduction rate by variation of expandable graphite's mesh size at double flame-retardant waste paper were secured through a cone calorimeter test. The thermal diffusion rate data of the specimen were secured through the LFA 1000 experiment. Through experiments, it has been confirmed that specimens using specific expandable graphite particles can be utilized as fire-resistant finishing materials in construction, ensuring fire resistance performance.

Keywords Wastepaper cellulose · Flame retardant · Th. diffusivity · ISO 5660-1 · LFA 1000 · Building finishing material

C. Ahn · D. Park
Department of Fire Safety Research, Korea Institute of Civil Engineering and Building Technology, Goyang 18544, Republic of Korea
e-mail: chansole@kict.re.kr

D. Park
e-mail: sunydong@inu.ac.kr

D. Park · Y. Kim
Graduate School of Safety Engineering, Incheon National University, Incheon 22012, Republic of Korea
e-mail: blue0772@inu.ac.kr

D. Rie (✉)
Fire Disaster Prevention Research Center, Incheon National University, Incheon, Republic of Korea
e-mail: riedh@inu.ac.kr

Introduction

High-rise and high-rise building construction is increasing as a countermeasure to solve residential spaces due to high density population concentration. According to research, the number of skyscrapers built worldwide over 200 m in 2018 was 148, indicating a 49.3% increase compared to 2013 (Qu et al. 2021), In Korea reported (2020), the number of buildings over 30 stories was 3165, a 52.5% increase compared to 1661 in 2016.

However, as the number of high-rise buildings increases, so do fire accidents that occur outside of these buildings (Bonner and Rein 2018, Bonner et al. 2020). In Korea reported (2017), the number of fires in buildings with 30 floors or more increased from 107 in 2014 to 145 in 2017, resulting in 11 times more casualties and 17 times more property damage due to fire accidents Flammable building finishes used in high-rise buildings were cited as the cause of increased fire casualties and property damage (Bonner et al. 2020; Bonner and Rein 2018). Table 1 illustrates fire accidents and damage caused by combustible building finishes in various countries worldwide.

In minimize the damage caused by fire spread due to combustible building finishes, countries worldwide have established regulations for building finishes fire performance to prevent fire expansion. Table 2 presents the safety standards for finishing material fire performance by major countries (Kodur et al 2022; NFPA 255 2006; Yoshioka et al 2021; Laban et al 2022; Kwark et al 2011; Korea Ministry of Land 2022).

Considering the laws regarding building finishes in various countries and the prevalence of fire accidents in high-rise buildings, it is crucial to develop fire-safe finishing building materials that can be applied to high-rise buildings, Therefore, several studies are being conducted to develop fire-safe finishing building materials. Table 3 shows various studies on flame retardant building finishes.

In a previous study aimed at developing flame-retardant building finishes, Wi et al. found that inorganic building finishes manufactured using recycled waste ceramics could reduce building energy consumption by 18.6% and improve the fire resistance performance of ceramics (Wi 2019). Wei et al. conducted experiments with formaldehyde-free poly siloxane coatings on Expanded Polystyrene (EPS) foam, which acted as adhesives and flame retardants. The EPS complex with the poly siloxane coating showed a 76% reduction in PHRR (Peak Heat Release Rate) and significantly reduced smoke

Table 1 Fire accidents caused by Combustible Building Finishing Materials

Date	Casualties		Number of Floors Affected by Fire	Fire Location	Country	Reference
	Death	Injury				
2015. 12	–	15	20	The Address Downtown	UAE	Barakat (2018) Chen et al. (2019)
2016. 06	–	–	12	Ramat Gan, a residential high- rise	Israel	WootLiff (2017)
2017. 06	80	70	24	Granfell Tower	U.K	Chen et al (2019)
2017. 12	29	37	9	Jecheon Sports Center	Korea	Ha et al (2022) Hwang et al (2020)
(2019. 02	–	1	6	Neo 200 building	Australia	James, O (2019)
2019. 11	–	27	1	The Cube Student Housing	U.K	Arewa et al (2021) Bahrami et al. (2022)
2020. 05	–	12	48	Abbco Tower	UAE	Arewa et al (2021) Ali (2020)
2020. 10	–	91	33	Ulsan mixed-use apartment	Korea	Woo et al. (2022)

Table 2 Comparison of regulations related to interior materials in each country

Country	Target	Test Standard	Classification
U.S.A	Building Interior Material	NFPA 255	Class A ~ C
Europe		EN 13501–1	A1, A2 ~ F Class
Korea & Japan		ISO 1182, ISO 5660–1, ISO 2271	Non-combustible-material Semi-noncombustible-material Fire Retardant-material

Table 3 Several studies on flame retardant building finishing materials

Contents	Reference
Assessment of recycled ceramic-based inorganic insulation for improving energy efficiency and flame retardancy of buildings	Wi et al. (2019)
A green, durable and effective flame-retardant coating for expandable polystyrene foams	Wei et al. (2022)
Flame-retardant and thermally-insulating tannin and soybean protein isolate (SPI) based foams for potential applications in building materials	Chen et al. (2022)
Fire propagation Characteristics and fire risks of polyurethanes: effects of material type (foam & board) and added flame retardant	Choi et al. (2022)
A Study on the Flame-Retardant Performance of Recycled Paper Building Materials Manufactured by 3D Printer	Hwang et al. (2022)

release compared to the existing EPS complex (Wi et al. 2019). Chen et al. developed a flame-retardant tannin-furan-SPI bio foam by adding boric acid and montmorillonite phosphate. The developed SPI bio foam was confirmed to have a PHRR value of 16.54 ~ 29.03 kW/m^2 through a cone calorimeter test, and the thermal conductivity of up to 0.0627W/m•K was measured, suggesting the possibility of making flame-retardant building materials (Wei et al. 2022). Choi et al. studied the differences in fire performance and toxicity between polyurethane foam & board (PUR-F, PUR-B) and polyisocyanurate foam & board (PIR-F, PIR-B) through ISO 5660-1, KS F 2271, and sill-sized fire. They concluded that further experiments with various flame retardants were needed (Chen et al. 2022). Hwang et al. produced a 3D printer to manufacture cellulose finishing materials and tested the ISO 11925-2 experiment for cellulose finishing materials. They found that cellulose finishing material with 20 wt% ceramic binder satisfies the vertical flame propagation length within 150 mm in the 30 s flame contact, the standard of EN 13501-1. They also found that the cellulose finishing material with 40 wt% ceramic binders did not have residual flames after the ISO 11925-2 experiment (Hwang et al. 2022). This research conducted experiments on a total of 5 expandable graphite particles sizes by adding two expandable graphite particles sizes as variables in addition to the expandable graphite with particle sizes added to the cellulose finishing material used in a prior research at Kim et al. (Kim et al. 2023) The change in fire performance and thermal diffusivity according to the change in expandable graphite particle size were verified through the ISO 5660-1 experiment and the LFA 1000 experiment. Figure 1 shows the flow chart of this study.

Description of specimens and test

Description of making specimens

The double flame-retardant mixed waste paper-based specimen used in this study was produced using an

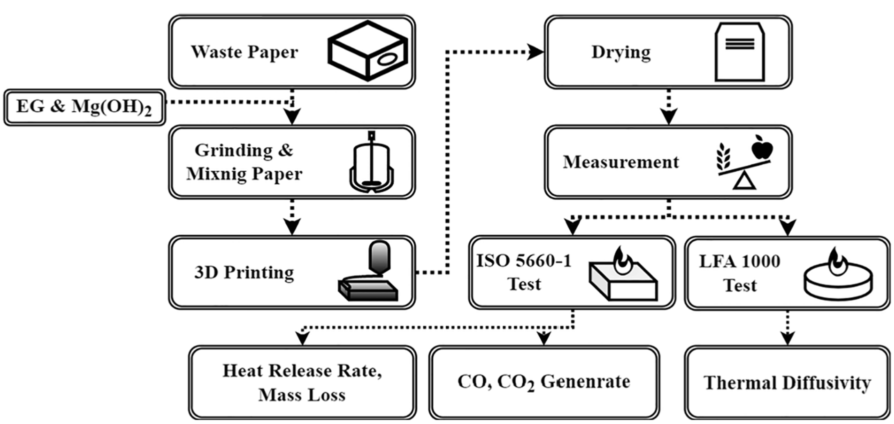

Fig. 1 Flowchart of this study design [28]

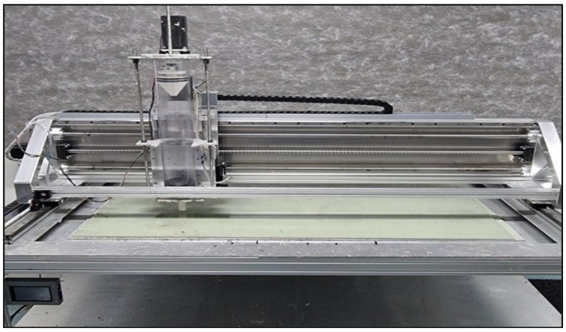

Fig. 2 Large Wet Cellulose (LWC)—3D Printer, Incheon National University Fire Disaster Prevention Research Center

LWC-3D printer with confirmed manufacturing efficiency and uniformity (Hwang et al. 2022; Ahn et al.2022). The LWC-3D printer was used to manufacture specimens with uniform fire performance. Figure 2 shows the LWC-3D printer used to manufacture the specimens.

In this study, Expandable Graphite (EG) and Magnesium Hydroxide (MH) flame retardants were added to enhance the fire performance of the cellulose building finish. The purpose of adding each flame retardant is as follows.

1. The addition of expandable graphite aims to protects the lower layer of the specimen to suppress the spread of external fire by expanding graphite during heating and forming a char layer. (Xia et al 2022; Chun et al. 2017).
2. Magnesium hydroxide was added to improve retardant performance through an endothermic reaction during the thermal reaction. The formula for the endothermic reaction of magnesium hydroxide is as follows Eq. (1) (Chung et al. 2011; Meucci et al. 2022).

$$Mg(OH)_2 \rightarrow MgO + H_2O1244 \sim 1450J/g \quad (1)$$

Two flame retardants (EG & MH) were added to the waste paper-based construction finishing material. Additionally, five different particle sizes of expandable graphite were added to the same content to analyze the fire performance based on the particle size variations. Table 4 shows the particle size of expandable graphite added to the cellulose flame retardant, while Table 5 shows the composition of waste paper-based specimens made of flame retardant building finishes.

Table 6 shows a photograph of the ISO 5660-1 specimen of the manufactured flame retardant construction finishing material.

Description of heat release rate test (ISO 5660–1)

Construction finishing materials must undergo a performance certification procedure to ensure their safety in case of fire. This research measures the heat release rate of the specimen by applying the ISO 5660–1 Cone Calorimeter test method. Radiant heat is continuously applied to samples located 22.5 mm away from the cone heater at a heat flow rate of 50 kW, and the heat release rate is calculated using the principle that approximately 13.1 MJ of heat is generated when 1 kg of oxygen is consumed during material

Table 4 Picture of expandable graphite particle size

Mesh	50	80	100	150	200
Particle Size (µm)	279 µm	173 µm	140 µm	104 µm	74 µm
Picture		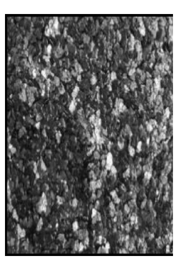	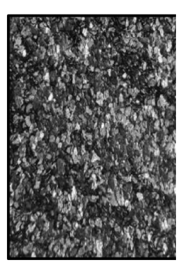	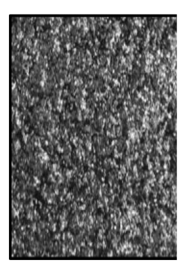	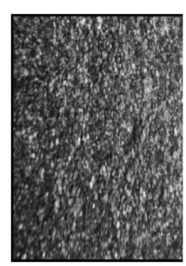

Table 5 Composition of specimens

Expandable graphite mesh	50mesh (279 μm)	80mesh (173 μm)	100mesh (140 μm)	150mesh (104 μm)	200mesh (74 μm)
Cellulose (waste paper)	100 g				
Expandable graphite	30 g				
$Mg(OH)_2$	20 g				

Table 6 Printed and after drying ISO 5660–1 specimen

Expandable graphite mesh	50mesh (279 μm)	80mesh (173 μm)	100mesh (140 μm)	150mesh (104 μm)	200mesh (74 μm)
Picture					

Fig. 3 International Organization for Standardization 5660–1 (Cone calorimeter)

combustion. The oxygen consumed is measured using an oxygen analyzer of a cone calorimeter, and the HRR (Heat Release Rate) is calculated through the measured amount of oxygen consumption using Eq. (2) (British Standard Institution 2021; Zhang et al 2015).

$$\dot{q} = E(\dot{m}_{O_2,0} - \dot{m}_{O_2}) \quad (2)$$

where:

$\dot{q}$ = Heat Release Rate (HRR).

E = The heat generated per unit mass of oxygen consumed E≒13.1 kJ/g_{O_2}

$\dot{m}_{O_2,0}$ = Mass flow rate of oxygen in the incoming air.

$\dot{m}_{O_2}$= Mass flow rate if oxygen in the exhaust gases.

Figure 3 shows the ISO 5660–1 Cone Calorimeter (FESTEC, Co, Korea) used in this experiment.

Figure 4 schematically shows the fire experiment part of the cone calorimeter equipment used in this experiment.

Table 7 shows the flame retardant and semi-non-combustible performance standards of the ISO 5660–1 test as specified by the International Organization for Standardization. This table serves as the standard for evaluating the flame retardant and semi-noncombustible experiments of the specimens (British Standard Institution 2021).

Fig. 4 Method of Test 5660–1 (Cone calorimeter)

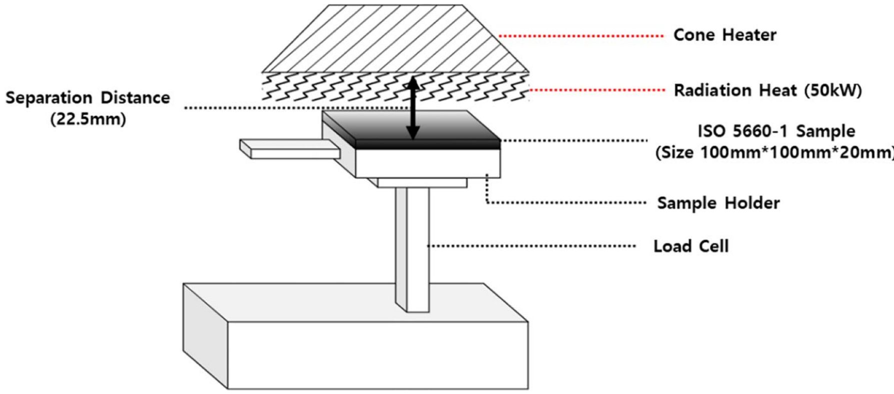

Table 7 Performance standard using the ISO 5660–1 test method

Standard	Class	Evaluation Criteria
ISO 5660-1 (Cone Calorimeter Method)	Semi-non-combustible Material	1. Total Radiant Heat 10 min after Heating is 8 MJ/m^2 within 10 min 2. Max. Heat Radiant Rate does not exceed 200 kW/m^2 for longer than 10 Consecutive Seconds 3. There shall be no crack that penetrates sample, ole or Melting (for Mixed Content Materials, includes melting and dissipating of all core materials) after heating for 10 min
	Fire retardant material	1. Total Radiant Heat 5 min after heating is 8 MJ/m^2 within 5 min 2. Max. Heat Radiant Rate does not exceed 200 kW/m^2 for Longer than 10 Consecutive Seconds 3. There shall be not Crack that penetrates sample, hole or melting (for Mixed Content Materials, includes Melting and Dissipating of all Core Materials) after heating for 5 min

Description of thermal diffusivity test (LFA 1000 test)

The thermal diffusivity of the cellulose produced was measured using LFA (Laser Flash Analysis) 1000 experimental equipment. Figure 5 shows the LFA 1000 equipment used to measure the thermal diffusivity.

The LFA 1000 experiment follows the method proposed by Parker in 1961 (Vitiello et al 2021; ASTM International 2013; Parker et al 1961). The test method utilizes the principle that the absorbed heat energy is transferred to the rear surface of the specimen by irradiating a laser flash on the front surface of the test object. The temperature rise at the rear of the specimen is measured over time until it reaches and saturates at the maximum temperature. Figure 6 shows the Laser Flash method used in the LFA 1000 experimental equipment.

The ratio of temperature changes over time measured by the method shown in Fig. 6 is calculated according to Eq. (3) of the thermal diffusivity calculation proposed by Parker (Parker et al 1961).

$$\alpha = 0.13879L^2/t_{1/2} \quad (3)$$

Fig. 5 LFA 1000 of Department of Fire Safety Research, Korea Institute of Civil Engineering and Building Technology

where:
α: Thermal Diffusivity [cm^2/s].
L: Thick of Specimens [cm].
$t_{1/2}$: The Time taken to increase to the 50% Point in the Graph of the Temperature increase of the Opposite Surface [s].

Test result and discussion

Result of ISO 5660–1

In order to confirm the fire performance of cellulose manufactured with each particle size of expandable graphite, an ISO 5660–1 experiment was conducted three times for each specimen to confirm the uniformity of the specimen's fire performance.

Figure 7 shows the trend change of HRR due to the difference in particle size of expandable graphite, as measured by conducting the test three times.

Figure 8 shows the difference in THR (Total Heat Release) values resulting from the difference in particle size of expandable graphite, as measured by conducting a test three times per specimen.

Figure 9 illustrates the values obtained by conducting a test three times for each specimen to verify the amount of carbon monoxide generated due to the difference in particle size of expandable graphite.

Figure 10 shows the value obtained by conducting a test three times for each specimen to confirm the amount of carbon dioxide generated due to the difference in particle size of expandable graphite.

Figure 11 shows the value obtained by conducting three tests of the mass reduction of the specimen during the cone calorimeter test process according to the particle size of expandable graphite.

Table 8 summarizes and shows the results of the cone calorimeter experiment according to the change in particle size of expandable graphite.

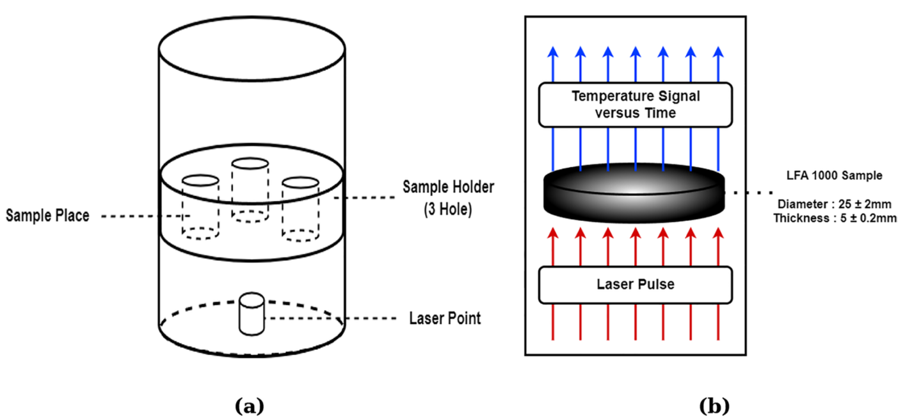

Fig. 6 **a** Illustrative diagram LFA 1000 Test **b** Laser Flash Analysis Method

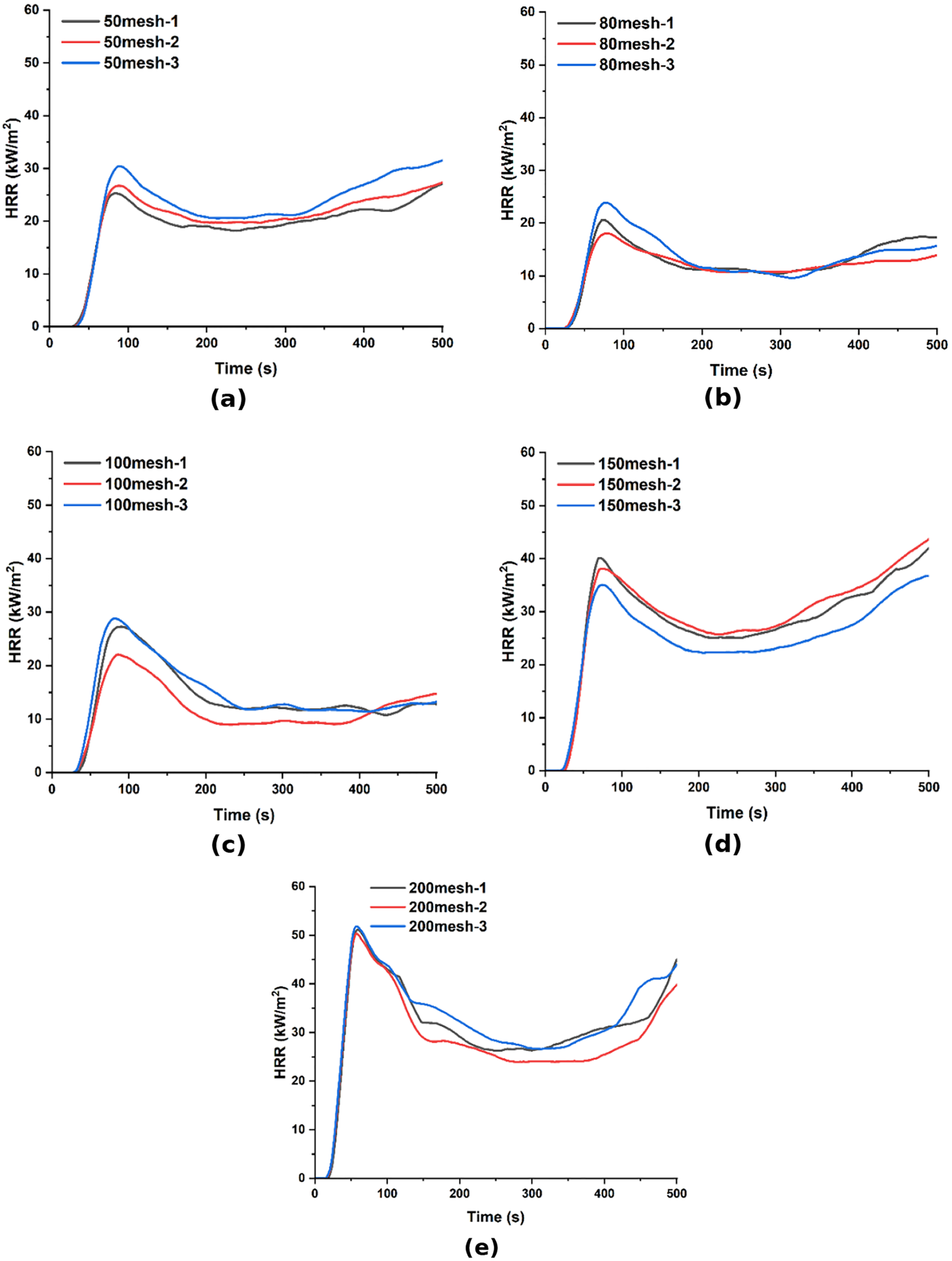
50mesh-1
50mesh-2
50mesh-3
HRR (kW/m²)
Time (s)
(a)
80mesh-1
80mesh-2
80mesh-3
HRR (kW/m²)
Time (s)
(b)
100mesh-1
100mesh-2
100mesh-3
HRR (kW/m²)
Time (s)
(c)
150mesh-1
150mesh-2
150mesh-3
HRR (kW/m²)
Time (s)
(d)
200mesh-1
200mesh-2
200mesh-3
HRR (kW/m²)
Time (s)
(e)

◂**Fig. 7** HRR measurement of all specimens **a** mesh 50 (279 μm) **b** mesh 80 (173 μm) **c** mesh 100 (140 μm) **d** mesh 150 (104 μm) **e** mesh200 (74 μm)

Result of LFA 1000

To investigate the effect of expandable graphite particle size on the thermal diffusion rate of cellulose material, three LFA 1000 tests were conducted at 20°C with the particle size as a variable. The thermal diffusion rate was measured, and uniformity was verified. Table 9 summarizes the results of the thermal diffusion rate experiment according to the changes in expandable graphite particle size.

Discussion

Through the ISO 5660-1 test and the LFA 1000 test, the effect of a change in the particle size of expandable graphite on the fire performance and thermal diffusion rate of cellulose materials was confirmed.

Figure 12 shows the distribution and trend line of PHRR according to the particle size of expandable graphite.

As a result of analyzing the PHRR, it was confirmed that the lowest PHRR value was observed with the particle size of 173 μm for expandable graphite, and all of the flame-retardant performance standards of PHRR 200 kW/m^2 or less were satisfied.

Figure 13 shows the distribution and trend line of THR at 300 s according to the expandable graphite particle size.

As a result of analyzing the THR at 300 s, it was confirmed that the average THR was the lowest for the particle size of expandable graphite at 173 μm, and flame-retardant performance was confirmed for particle sizes of 104 μm, 140 μm, 173 μm, and 279 μm..

Figure 14 shows the distribution and trend line of THR at 500s according to the expandable graphite particle size.

As a result of analyzing the THR at 500s, it was confirmed that the average THR was the lowest when the particle size of expandable graphite was 173 μm.

Figure 15 depicts the distribution and trend line of toxic gas CO and CO_2 generation in relation to the particle size of expandable graphite, and the Toxic Index was calculated based on the lowest published lethal concentration (LCLO) as defined by the NIOSH (National Institute of Occupational Safety and Health), using CO: 5,000 ppm (human, 5min) and CO_2: 90,000 ppm (human, 5min).

As a result of analyzing CO and CO_2 production amounts, the lowest average CO production amount at the particle size of expandable graphite of 104 μm was confirmed, and the lowest average CO_2 production amount at the particle size of expandable graphite of 140 μm was confirmed. In addition, as a result of calculating the index values of CO and CO_2 based on the minimum lethal concentration stipulated by the National Institute of Occupational Safety and Health (NIOSH), a low Toxic Index value was confirmed at a particle size of 140 to 173 μm. The calculations of the CO and CO_2 Index values are shown in Eqs. 3 and 4, and the Toxic Index was calculated as shown in Eq. 5.

$$COIndex = \frac{COGenerate/500sec}{CO_{LC}/300sec} \tag{4}$$

$$CO_2Index = \frac{CO_2Generate/500sec}{CO_{2,LC}Generate/300sec} \tag{5}$$

$$ToxicIndex = COIndex + CO_2Index \tag{6}$$

Figure 16 shows the distribution and trend line of mass loss according to the particle size of expandable graphite.

As a result of mass reduction data analysis, the lowest average mass reduction in the expandable graphite particle size of 140 μm was confirmed, and as the particle size of expandable graphite increased, the mass reduction decreased and then increased again in the particle size of 180 μm ~ 279 μm.

Figure 17 illustrates the distribution and trend line of data measured in the LFA 1000 experiment for thermal diffusivity at 20 °C as a function of the expandable graphite particle size.

The LFA 1000 Test was conducted at a temperature of 20℃, and it was verified that, as the particle size of expandable graphite increased, the thermal diffusion rate decreased.

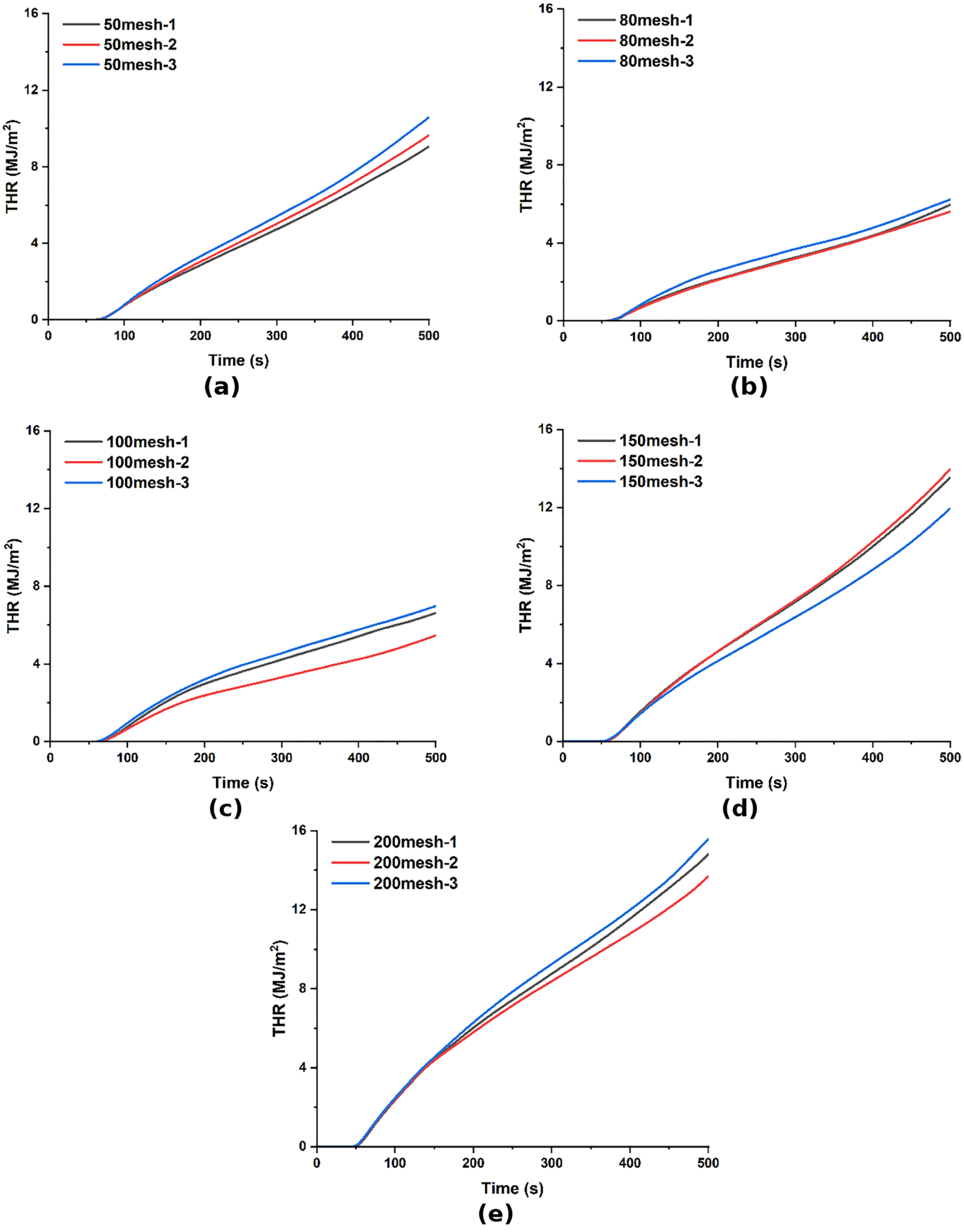

Fig. 8 THR measurement of all specimens **a** mesh 50 (279 μm) **b** mesh 80 (173 μm) **c** mesh 100 (140 μm) **d** mesh 150 (104 μm) **e** mesh200 (74 μm)

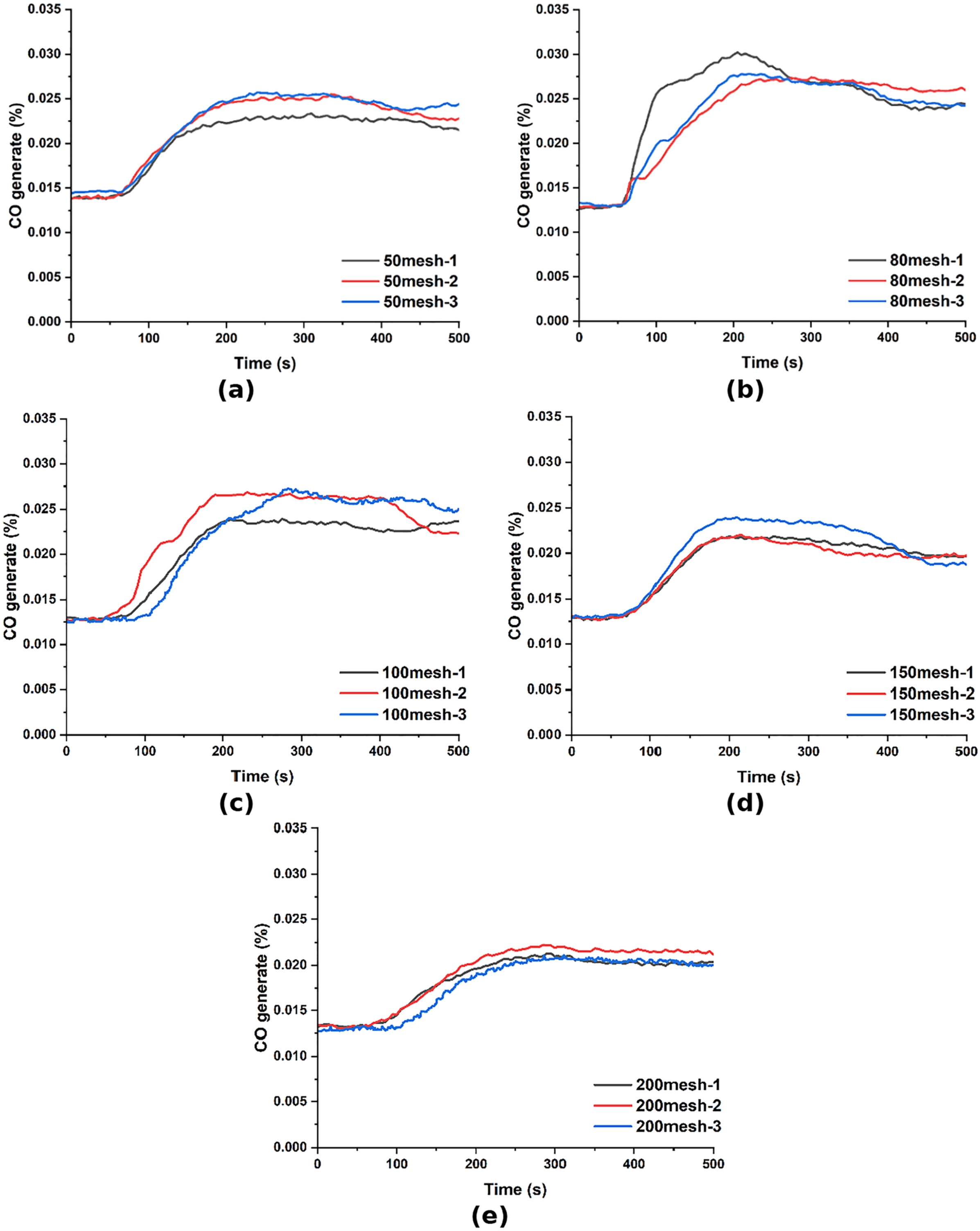

Fig. 9 CO generate of all specimens **a** mesh 50 (279 μm) **b** mesh 80 (173 μm) **c** mesh 100 (140 μm) **d** mesh 150 (104 μm) **e** mesh200 (74 μm)

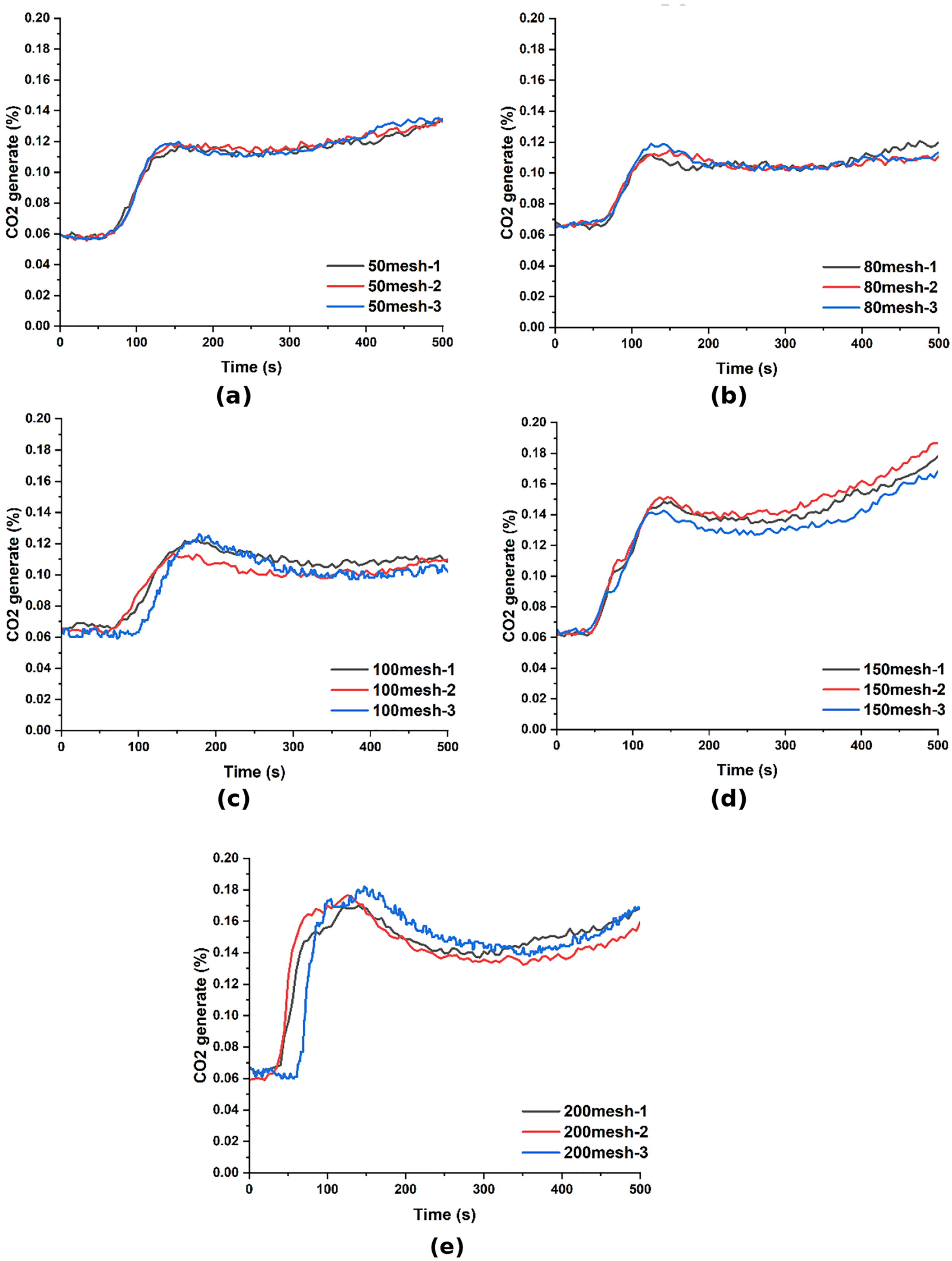

Fig. 10 CO_2 generate of all specimens **a** mesh 50 (279 μm) **b** mesh 80 (173 μm) **c** mesh 100 (140 μm) **d** mesh 150 (104 μm) **e** mesh200 (74 μm)

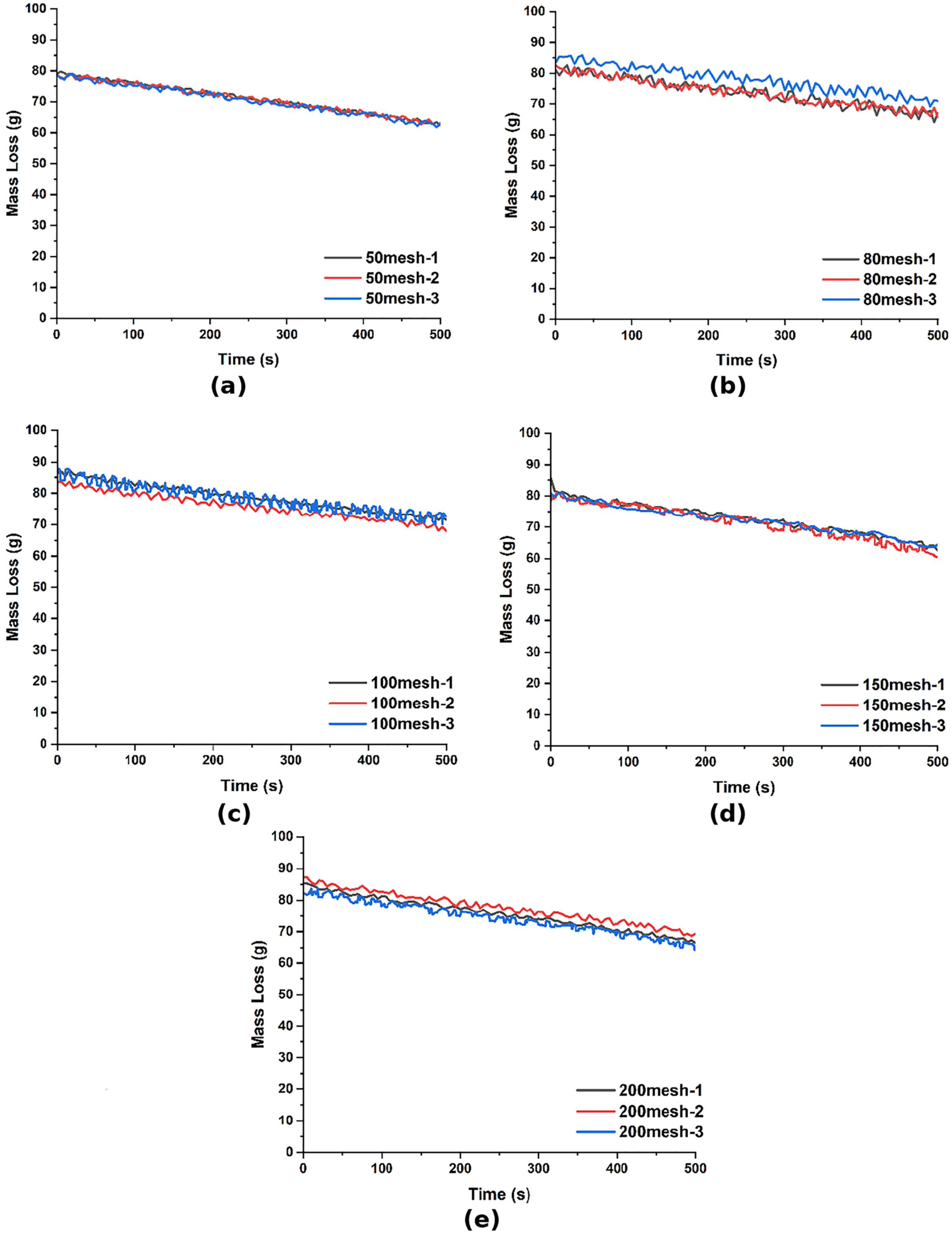

Fig. 11 Mass Loss of all specimens at ISO 5660–1 test **a** mesh 50 (279 µm) **b** mesh 80 (173 µm) **c** mesh 100 (140 µm) **d** mesh 150 (104 µm) **e** mesh200 (74 µm)

Table 8 ISO 5660–1 Test Result on PHRR, THR at 300 s THR at 500 s, CO, CO_2 Generate, Mass Loss

EG Particle Size	No	PHRR (kW/m^2)	THR (MJ/m^2)		Toxic Gas Generate		Mass Loss (g)
			at 300 s	at 500 s	CO_2 (%)	CO (%)	
50mesh (279 μm)	1	31.9	4.727	9.058	0.078	0.0068	19.26
	2	35.87	5.021	9.645	0.087	0.0100	20.5
	3	41.55	5.404	10.582	0.095	0.0086	19.33
80mesh (173 μm)	1	22.22	3.261	5.962	0.055	0.0118	19.26
	2	18.7	3.203	5.613	0.052	0.0119	20.81
	3	24.92	3.689	6.231	0.054	0.0118	15.96
100mesh (140 μm)	1	27.8	4.229	6.642	0.052	0.0091	17.39
	2	22.59	3.313	5.504	0.054	0.0084	16.68
	3	29.43	4.555	6.999	0.054	0.0107	17.56
150mesh (104 μm)	1	41.99	7.154	13.55	0.120	0.0071	22.2
	2	43.66	7.254	13.975	0.143	0.0065	22.02
	3	36.76	6.367	11.95	0.115	0.0064	21.54
200mesh (74 μm)	1	51.19	8.754	14.81	0.151	0.0078	23.45
	2	50.38	8.379	13.686	0.152	0.0070	21.85
	3	51.82	9.251	15.574	0.137	0.0073	21.07

Table 9 LFA1000 Test Result on Thermal Diffusivity

EG Particle Size (μm)	No	Thermal Diffusivity (cm^2/s)
50mesh (279 μm)	1	0.0025
	2	0.0025
	3	0.0024
80mesh (173 μm)	1	0.0029
	2	0.0029
	3	0.003
100mesh (140 μm)	1	0.0039
	2	0.0038
	3	0.0038
150mesh (104 μm)	1	0.0044
	2	0.0042
	3	0.0044
200mesh (74 μm)	1	0.0052
	2	0.005
	3	0.0051

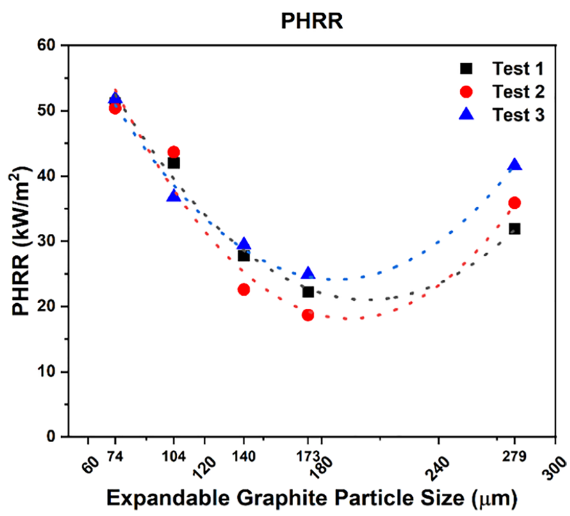

Fig. 12 PHRR Distribution and Trend line by Expandable Graphite particle size

Conclusion

To determine the effect of expandable graphite particle size on the fire performance and thermal diffusivity of the cellulose materials manufactured by the LWC-3D printer, ISO 5660–1 heat release and LFA 1000 thermal diffusivity tests were conducted, leading to the following conclusions:

1. Cellulose finishing materials manufactured with LWC-3D printers have uniform Peak heat release and Total heat release, as well as uniform CO, CO_2 generation, Mass loss, and Thermal Diffusivity.

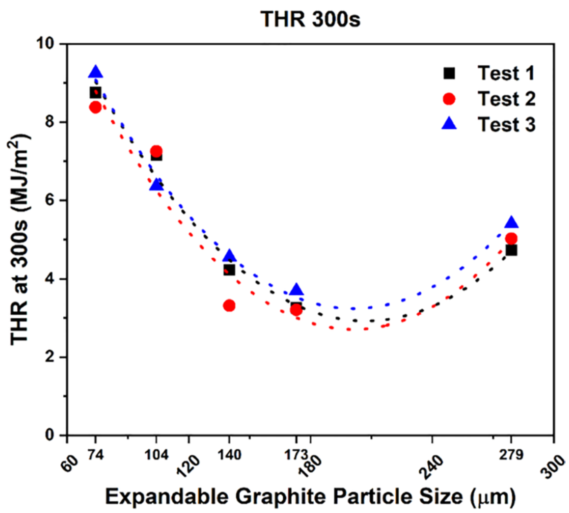

Fig. 13 THR at 300 s Distribution and Trend line by Expandable Graphite particle size

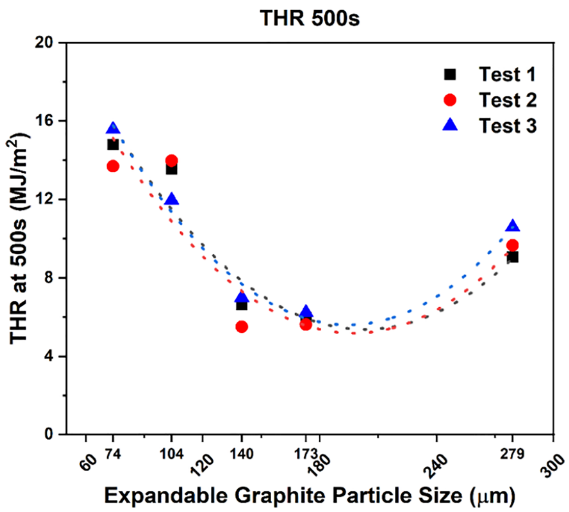

Fig. 14 THR at 500 s Distribution and Trend line by Expandable Graphite particle size

2. The ISO 5660–1 test was conducted on five specimens with different expandable graphite particle sizes, and it was confirmed that the PHRR and THR were the lowest with the expandable graphite particle size of 173 µm.
3. Cellulose finishes produced in the ratio of 100g of cellulose, 30g of expandable graphite, and 20g of magnesium hydroxide met the flame retardant performance standards required by the ISO 5660–1 test in the range of 104 µm to 279 µm in particle size, and can be used as a building finishing material with flame retardant performance.
4. The ISO 5660–1 test results show that the amount of CO produced and CO_2 produced changed as the THR decreased with the size of the expandable graphite particles. The particle size change of expandable graphite added to the cellulose finishing material manufactured by calculating the Toxic Index for CO and CO_2 production affected the combustion gas production amount and the Toxic Index.
5. A comprehensive analysis of ISO 5660–1 test results showed that the section with the best fire performance was 140 µm to 173 µm, and the inflection point of the fire performance was shown from the particle size of 173 µm or more.
6. Analyzing the change in thermal diffusion rate through the LFA 1000 thermal diffusion rate measurement test confirmed that the increase in particle size of the added expandable graphite leads to a decrease in thermal diffusion rate of the cellulose construction finishing material, and basic data on insulation performance were secured by securing data on the change in thermal diffusivity as the particle size of expandable graphite increased.

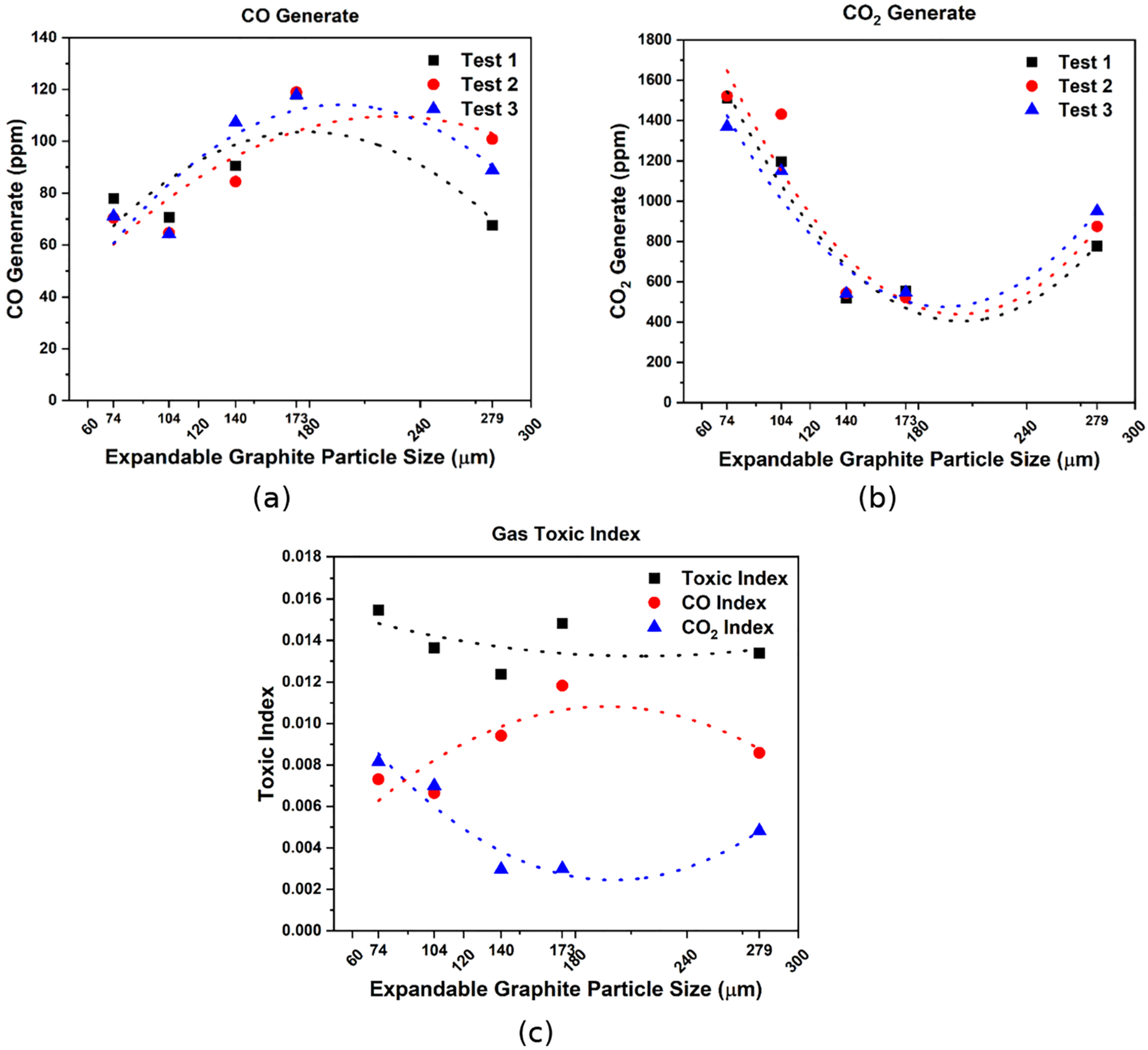

Fig. 15 Toxic Gas Distribution and Trend line by Expandable Graphite particle size **a** CO Generate **b** CO_2 Generate **c** Toxic Index Average

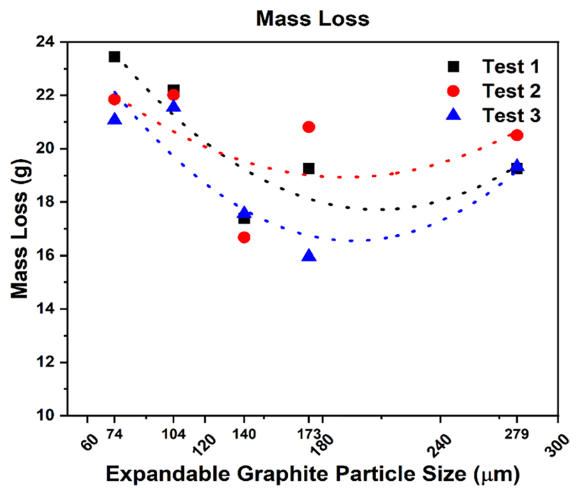

Fig. 16 Mass Loss Distribution and Trend line by Expandable Graphite particle

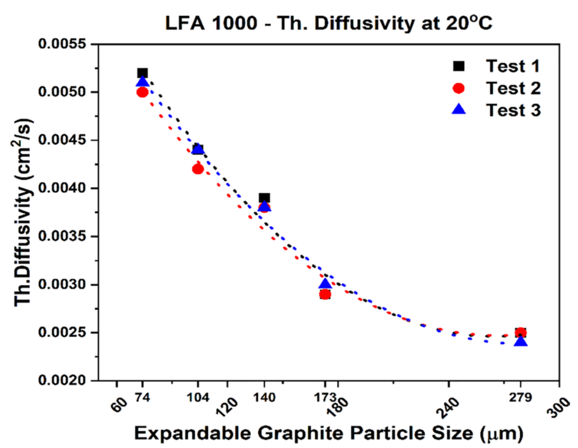

Fig. 17 Test of LFA 1000 Thermal Diffusivity at 20 °C Distribution and Trend line by Expandable Graphite particle

Acknowledgements This work is supported by the Korea Agency for Infrastructure Technology Advancement (KAIA) grant funded by the Ministry of Land, Infrastructure and Transport (Grant RS-2021-KA163162)

Author contributions Conceptualization, DR; Methodology, DR; Software, DP; Validation, DP; Analysis, CA and DP; Resources, DP; Writing, DP and YK; Review & Editing, DR and DP; Visualization, DP; Supervision, DR; Project Administration, DR; Funding Acquisition, CA.

Funding This work is supported by the Korea Agency for Infrastructure Technology Advancement (KAIA) grant funded by the Ministry of Land, Infrastructure and Transport (Grant RS-2021-KA163162).

Data availability Available upon request.

Declarations

Conflict of interest The authors declare no conflict of interest.

References

Ahn C, Park D, Hwang J, Rie D (2022) A study on the reliability of mass, density, and fire performance of recycled wastepaper building finishing material made with large wet cellulose 3D printers. Sustainability 14:13090. https://doi.org/10.3390/su142013090

Ali A (2020) Sharjah's fire-hit Abbco building was fitted with banned cladding. IOP publishing gulfnews https://gulfnews.com/uae/sharjahs-fire-hit-abbco-building-was-fitted-with-banned-cladding-1.71357 Accessed on 6 may 2020

Arewa AO, Ahmed A, Edwards DJ, Nwankwo C (2021) Fire safety in high-rise buildings: is the stay-put tactic a misjudgement or magnificent strategy? Buildings 11:339. https://doi.org/10.3390/buildings11080339

ASTM International (2013) Standard test method for thermal diffusivity by the flash method 1, E1vols. ASTM Int 461–13:1–11

Bahrami S, Zeinali D (2022) The sustainability challenge of product information quality in the design and construction of facades: lessons from the Grenfell Tower fire. Smart Sustain Built Environ 12(3):488–506. https://doi.org/10.1108/SASBE-06-2021-0100

Barakat N (2018) Fire at Address hotel on New Year's Eve Caused by Electrical Fault: Dubai Police. IOP publishing gulfnews https://gulfnews.com/news/uae/emergencies/fire-at-address-hotel-on-new-year-seve-caused-by-electrical-fault-dubai-police-1.1656786 Accessed 8 July 2018

Bonner M, Rein G (2018) Flammability and multi-objective performance of building façades: towards optimum design. Int J High-Rise Build 7(4):363–374

Bonner M, Wegrzynski W, Papis BK, Rein G (2020) KRESNIK: a top-down, statistical approach to understand the fire performance of building facades using standard test data. Build Environ 169:106540

British Standards Institution Reaction-to-Fire Tests. (2021) Heat Release, Smoke Production and Mass Loss Rate. Part 1, Heat Release Rate (Cone Calorimeter Method) and Smoke Production Rate (Dynamic Measurement).;

Chen TBY, Yuen ACY, Yeoh GH, Yang W, Chan QN (2019) Fire risk assessment of combustible exterior cladding using a collective numerical database. Fire 2:11. https://doi.org/10.3390/fire2010011

Chen X, Li J, Essawy H, Pizzi A, Fredon E, Gerardin C, Zhou X (2022) Flame-retardant and thermally-insulating tannin and soybean protein isolate (SPI) based foams for potential applications in building materials. Constr Build Mater 315:125711

Choi JH, Chae SU, Hwang EH, Choi DM (2022) Fire propagation characteristics and fire risks of polyurethanes: effects of material type (foam & board) and added flame retardant. Fire 5(4):105

Chun KO, Rie DH (2017) A study for the fire retardant-characteristics of expandable graphite composite materials. J Korean Soc Saf 32(3):28–33. https://doi.org/10.14346/JKOSOS.2017.32.3.28

Chung YJ, Lim HM, Jin E, Oh J (2011) Combustion-retardation properties of low density polyethylene and ethylene vinyl acetate mixtures with magnesium hydroxide. Appl Chem Eng 22(4):439–443

Ha J, Kim HJ, Kim JH, Park D (2022) Experience of disaster response team in jecheon sports center fire. J Korean Soc Integr Med 10(1):39–48

Hakkarainen T, Hayashi Y (2001) Comparison of Japanese and European fire classification systems for surface linings. Fire Sci Technol 21(1):19–42. https://doi.org/10.3210/fst.21.19

Hwang W, Shin H, Yang J (2020) Study on improved measures for fire safety management in sports facilities. J Korean Soc Hazard Mitig 20(3):139–147

Hwang J, Park D, Kim S, Rie D (2022) A study on the flame-retardant performance of recycled paper building materials manufactured by 3d printer. Sustainability 14:4798. https://doi.org/10.3390/su14084798

James O (2019) Cladding risks raised by Melbourne fire brigade before Neo200 blaze, but council deemed risk 'low'. IOP publishing ABC news https://www.abc.net.au/news/2019-06-23/melbourne-city-councilneo200-advice-before-fire-at-tower/11225992 Accessed on 23 June 2019

Kim Y, Park D, Rie D (2023) Evaluation of the flame-retardant performance and fire risk of cellulose building finishing material due to the particle size of expandable graphite. Sustainability 15:5426. https://doi.org/10.3390/su15065426

Kodur V, Venkatachari S, Matsagar VA, Singh SB (2022) Test methods for characterizing the properties of fiber-reinforced polymer composites at elevated temperatures. Polymers 14:1734. https://doi.org/10.3390/polym14091734

Kwark J-H, Choi J-M, Ku J-H (2011) A Study on evaluation methods for the fire-retardant performance of hanok components". Fire Sci Eng 25(5):1–7

Laban M, Ilić S, Džolev I, Draganić S (2022) European and national assessment procedure for the fire performance of facades. In Proceedings of the 19th International Symposium MASE, Ohrid, pp. 577–582.

Meucci M, Haveriku S, Badalassi M, Cardelli C, Ruggeri G, Pucci A (2022) Effect of polyolefin elastomers' characteristics and natural magnesium hydroxide content on the properties of halogen-free flame-retardant polyolefin composites". Micro 2:164–182. https://doi.org/10.3390/micro2010011

Ministry of Land (2022) Infrastructure and Transport. Code for the Flame - Retardant Performance of Building Finishing Materials and the Fire Preventing Structure, No. 2022-1106. https://www.law.go.kr/admRulLsInfoP.do?chrClsCd=&admRulSeq=2100000195901

National Fire Protection Association (2006) NFPA 255; Standard Method of Test of Surface Burning Characteristics of Building Materials. Quincy, MA, USA

Parker WJ, Jenkins RJ, Butler CP, Abbott GL (1961) Flash method of determining thermal diffusivity, heat capacity, and thermal conductivity. J Appl Phys 32(9):1679–1684. https://doi.org/10.1063/1.1728417

Qu J, Wang Z, Du P (2021) Comparative study on the development trends of high-rise buildings above 200 meters in China, the USA and the UAE. International J High-Rise Build 10(1):63–71

Republic of Korea National Fire Agency (2017) Fire Statistical Yearbook. Republic of Korea National Fire Agency, Sejong, Korea

Republic of Korea National Fire Agency (2020) Fire Statistical Yearbook. Republic of Korea National Fire Agency, Sejong, Korea

Vitiello D, Nait-Ali B, Tessier-Doyen N, Tonnesen T, Laím L, Rebouillat L, Smith DS (2021) Thermal conductivity of insulating refractory materials: comparison of steady-state and transient measurement methods. Open Ceramics 6:100118. https://doi.org/10.1016/j.oceram.2021.100118

Wi S, Yang S, Berardi U, Kim S (2019) Assessment of recycled ceramic-based inorganic insulation for improving energy efficiency and flame retardancy of buildings. Environ Int 130:104900

Woo B, Kim HK (2022) Regression analysis of delay in fire mobilization: focused on Busan metropolitan city. J Korean Soc Transp 40(1):99–110

WootLiff R (2017) Hundreds of Israeli buildings 'as vulnerable' as London's Grenfell Tower. IOP publishing Times of Israel https://www.timesofisrael.com/hundreds-israeli-buildings-as-vulnerable-as-londons-grenfell-tower/ Accessed 26 June 2017

Xia Y, Chai W, Liu Y, Su X, Liao C, Gao M, Zheng Z (2022) Facile fabrication of starch-based, synergistic intumescent and halogen-free flame retardant strategy with expandable graphite in enhancing the fire safety of polypropylene. Ind Crops Prod 184:115002

Yoshioka H, Noguchi T, Kobayashi K, Kanematsu M, Ando T, Pareek S, Hayakawa T (2021) Development of a new intermediate-scale box test on sandwich panel products compared with ISO 13784–1 room test and EN 13501–1 classification system. Fire Mater 45(8):1025–1034

Zhang W, Chen X, Chen Q, Ding C, Liu J, Chen M, Wang J (2015) Combustion calorimetry of carbonate electrolytes used in lithium ion batteries. J Fire Sci 33(1):22–36

Zhao W, Zhao HB, Cheng JB, Li W, Zhang J, Wang YZ (2022) A green, durable and effective flame-retardant coating for expandable polystyrene foams. Chem Eng J 440:135807